ENABLING DEEP SPIKING NEURAL NETWORKS WITH HYBRID CONVERSION AND SPIKE TIMING DEPENDENT BACKPROPAGATION

Anonymous authors
Paper under double-blind review

ABSTRACT

Spiking Neural Networks (SNNs) operate with asynchronous discrete events (or spikes) which can potentially lead to higher energy-efficiency in neuromorphic hardware implementations. Many works have shown that an SNN for inference can be formed by copying the weights from a trained Artificial Neural Network (ANN) and setting the firing threshold for each layer as the maximum input received in that layer. These type of converted SNNs require a large number of time-steps to achieve competitive accuracy which diminishes the energy savings. The number of time-steps can be reduced by training SNNs with spike-based backpropagation from scratch, but that is computationally expensive and slow. To address these challenges, we present a computationally-efficient training technique for deep SNNs. We propose a hybrid training methodology: 1) take a converted SNN and use its weights and thresholds as an initialization step for spike-based backpropagation, and 2) perform incremental spike-timing dependent backpropagation (STDB) on this carefully initialized network to obtain an SNN that converges within few epochs and requires fewer time-steps for input processing. STDB is performed with a novel surrogate gradient function defined using neuron's spike time. The weight update is proportional to the difference in spike timing between the current time-step and the most recent time-step the neuron generated an output spike. The SNNs trained with our hybrid conversion-and-STDB training perform at $10X - 25X$ fewer number of time-steps and achieve similar accuracy compared to purely converted SNNs. The proposed training methodology converges in less than 20 epochs of spike-based backpropagation for most standard image classification datasets, thereby greatly reducing the training complexity compared to training SNNs from scratch. We perform experiments on CIFAR-10, CIFAR-100 and ImageNet datasets for both VGG and ResNet architectures. We achieve top-1 accuracy of 65.19% for ImageNet dataset on SNN with 250 time-steps, which is $10X$ faster compared to converted SNNs with similar accuracy.

1 INTRODUCTION

In recent years, Spiking Neural Networks (SNNs) have shown promise towards enabling low-power machine intelligence with event-driven neuromorphic hardware. Founded on bio-plausibility, the neurons in an SNN compute and communicate information through discrete binary events (or spikes) that is a significant shift from the standard artificial neural networks (ANNs), which process data in a real-valued (or analog) manner. The binary all-or-nothing spike-based communication combined with sparse temporal processing precisely make SNNs a low-power alternative to conventional ANNs. With all its appeal for power efficiency, training SNNs still remains a challenge. The discontinuous and non-differentiable nature of a spiking neuron (generally, modeled as leaky-integrate-and-fire (LIF), or integrate-and-fire (IF)) poses difficulty to conduct gradient descent based backpropagation. Practically, SNNs still lag behind ANNs, in terms of performance or accuracy, in traditional learning tasks. Consequently, there has been several works over the past few years that propose different learning algorithms or learning rules for implementing deep convolutional SNNs for complex visual recognition tasks (Wu et al., 2019; Hunsberger & Eliasmith,

2015; Cao et al., 2015). Of all the techniques, conversion from ANN-to-SNN (Diehl et al., 2016; 2015; Sengupta et al., 2019; Hunsberger & Eliasmith, 2015) has yielded state-of-the-art accuracies matching deep ANN performance for Imagenet dataset on complex architectures (such as, VGG (Simonyan & Zisserman, 2014) ResNet (He et al., 2016)). In conversion, we train an ANN with ReLU neurons using gradient descent and then convert the ANN to an SNN with IF neurons by using suitable threshold balancing (Sengupta et al., 2019). But, SNNs obtained through conversion incur large latency of 2000-2500 time steps (measured as total number of time-steps required to process a given input image[1]). The large latency translates to higher energy consumption during inference thereby diminishing the efficiency improvements of SNNs over ANNs. To reduce the latency, spike-based backpropagation rules have been proposed that perform end-to-end gradient descent training on spike data. In spike-based backpropagation methods, the non-differentiability of the spiking neuron is handled by either approximating the spiking neuron model as continuous and differentiable (Huh & Sejnowski, 2018) or by defining a surrogate gradient as a continuous approximation of the real gradient (Wu et al., 2018; Bellec et al., 2018; Neftci et al., 2019). Spike-based SNN training reduces the overall latency by $\sim 10\times$ (for instance, 200-250 timesteps required to process an input (Lee et al., 2019)) but requires more training effort (in terms of total training iterations) than conversion approaches. A single feed-forward pass in ANN corresponds to multiple forward passes in SNN which is proportional to the number of time-steps. In spike-based backpropagation, the backward pass requires the gradients to be integrated over the total number of time-steps that increases the computation and memory complexity. The multiple-iteration training effort with exploding memory requirement (for backward pass computations) has limited the applicability of spike-based backpropagation methods to small datasets (like CIFAR10) on simple few-layered convolutional architectures.

In this work, we propose a hybrid training technique which combines ANN-SNN conversion and spike-based backpropagation that reduces the overall latency as well as decreases the training effort for convergence. We use ANN-SNN conversion as an initialization step followed by spike-based backpropagation incremental training (that converges to optimal accuracy with few epochs due to the precursory initialization). Essentially, our hybrid approach of taking a converted SNN and incrementally training it using backpropagation yields improved energy-efficiency as well as higher accuracy than a model trained from scratch with only conversion or only spike-based backpropagation.

In summary, this paper makes the following contributions:

- We introduce a hybrid computationally-efficient training methodology for deep SNNs. We use the weights and firing thresholds of an SNN converted from an ANN as the initialization step for spike-based backpropagation. We then train this initialized network with spike-based backpropagation for few epochs to perform inference at a reduced latency or time-steps.

- We propose a novel spike time-dependent backpropagation (STDB, a variant of standard spike-based backpropagation) that computes surrogate gradient using neuron's spike time. The parameter update is triggered by the occurrence of spike and the gradient is computed based on the time difference between the current time-step and the most recent time-step the neuron generated an output spike. This is motivated from the Hebb's principle which states that the plasticity of a synapse is dependent on the spiking activity of the neurons connected to the synapse.

- Our hybrid approach with the novel surrogate gradient descent allows training of large-scale SNNs without exploding memory required during spike-based backpropagation. We evaluate our hybrid approach on large SNNs (VGG, ResNet-like architectures) on Imagenet, CIFAR datasets and show near iso-accuracy compared to similar ANNs and converted SNNs at lower compute cost and energy.

The code to train and test the spiking network (using Pytorch framework) is available online [2].

---

[1]SNNs process Poisson rate-coded input spike trains, wherein, each pixel in an image is converted to a Poisson-distribution based spike train with the spiking frequency proportional to the pixel value (Sengupta et al., 2019)

[2]attached during submission for anonymity

2 SPIKE TIMING DEPENDENT BACKPROPAGATION (STDB)

In this section, we describe the spiking neuron model, derive the equations for the proposed surrogate gradient based learning, present the weight initialization method for SNN, discuss the constraints applied for ANN-SNN conversion, and summarize the overall training methodology.

2.1 LEAKY INTEGRATE AND FIRE (LIF) NEURON MODEL

The neuron model defines the dynamics of the neuron's internal state and the trigger for it to generate a spike. The differential equation

$$\tau \frac{dU}{dt} = -(U - U_{rest}) + RI \tag{1}$$

is widely used to characterize the leaky-integrate-and-fire (LIF) neuron model where, U is the internal state of the neuron referred as membrane potential, U_{rest} is the resting potential, R and I are the input resistance and current, respectively. The above equation is valid when the membrane potential is below the threshold value (V). The neuron geneartes an output spike when $U >= V$ and U is reduced to the reset potential. This representation is described in continuous
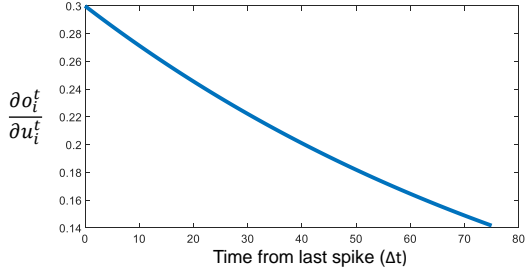

Figure 1: Surrogate gradient of the spiking neuron activation function (Eq. 11). $\alpha = 0.3, \beta = 0.01$. The gradient is computed for each neuron and Δt defines the time difference between current simulation time and the last spike of the neuron. For example, if a neuron spikes at $t_s = 12$ its gradient will be maximum at $t = 12(\Delta t = 0)$ and gradually decrease for later time-steps. If the same neuron spikes later at $t_s = 24$ its previous spike history will be overwritten and the gradient computation for $t = 24$ onward will only consider the most recent spike. This avoids the overhead of storing all the spike history in memory.

domain and more suitable for biological simulations. We modify the equation to be evaluated in a discrete manner in the Pytorch framework. The iterative model for a single post-neuron is described by

$$u_i^t = \lambda u_i^{t-1} + \sum_j w_{ij} o_j^t - v o_i^{t-1} \tag{2}$$

$$o_i^{t-1} = \begin{cases} 1, & \text{if } u_i^{t-1} > v \\ 0, & \text{otherwise} \end{cases} \tag{3}$$

where u is the membrane potential, subscript i and j represent the post- and pre-neuron, respectively, superscript t is the time-step, λ is a constant (< 1) responsible for the leak in membrane potential, w is the weight connecting the pre- and post-neuron, o is the binary output spike, and v is the firing threshold potential. The right hand side of Equation 2 has three terms: first term calculates the leak in the membrane potential from previous time-step, second term integrates the input from the previous layer and adds it to the membrane potential, third term which is outside the summation reduces the membrane potential by the threshold value if a spike is generated. This is known as soft reset as the membrane potential is lowered by v compared to hard reset where the membrane potential is reduced to the reset value. Soft reset enables the spiking neuron to carry forward the excess potential above the firing threshold to the following time-step, thereby minimizing information loss.

2.2 SPIKE TIMING DEPENDENT BACKPROPAGATION (STDB) LEARNING RULE

The neuron dynamics (Equation 2) show that the neuron's state at a particular time step recurrently depends on its state in previous time steps. This introduces implicit recurrent connections in the network (Neftci et al., 2019). Therefore, the learning rule has to perform the temporal credit assignment along with the spatial credit assignment. Gradient-descent learning solves both the credit assignment problem:

Algorithm 1 ANN-SNN Hybrid Initialization of parameters and threshold voltage

---

Input: Trained ANN model (A), SNN model (N), Input(X)
// Copy ann weights to snn
  for $l=1$ **to** L **do**
  | $N_l.W \leftarrow A_l.W$
  end
// Initialize threshold voltage to 0
  $V \leftarrow [0, \cdots, 0]_{L-1}$
  for $l=1$ **to** $L-1$ **do**
  | $v \leftarrow 0$
  | **for** $t=1$ **to** T **do**
  | | $O_0^t \leftarrow PoissonGenerator(X)$
  | | **for** $k=1$ **to** l **do**
  | | | **if** $k < l$ **then**
  | | | | // Forward (Algorithm 3)
  | | | **end**
  | | | **else**
  | | | | // Pre-nonlinearity (A)
  | | | | $A \leftarrow N_l(O_{k-1}^t)$
  | | | | **if** $max(A) > v$ **then**
  | | | | | $v \leftarrow max(A)$
  | | | | **end**
  | | | **end**
  | | **end**
  | **end**
  | $V[l] \leftarrow v$
  end

Algorithm 2 Initialize the neuron parameters. Membrane potential (U), last spike time (S), dropout mask (M). The initialization is performed once for every mini-batch.

Input: Input(X), network model(N)
$b\_size = X.b\_size$
  $h = X.height$
  $w = X.width$
  for $l=1$ **to** L **do**
  | **if** $isintance(N_l, Conv)$ **then**
  | | $U_l = zeros(b\_size, N_l.out, h, w)$
  | | $S_l = ones(b\_size, N_l.out, h, w) * (-1000)$
  | **end**
  | **else if** $isintance(N_l, Linear)$ **then**
  | | $U_l = zeros(b\_size, N_l.out)$
  | | $S_l = ones(b\_size, N_l.out) * (-1000)$
  | **end**
  | **else if** $isintance(N_l, Dropout)$ **then**
  | | // Generate the dropout map that will be fixed for all time steps
  | | $M_l = N_l(ones(U_{l-1}.shape))$
  | **end**
  | **else if** $isintance(N_l, AvgPool)$ **then**
  | | // Reduce the width and height after average pooling layer
  | | $h = h // kernel\_size$
  | | $w = w // kernel\_size$
  | **end**
  end

---

spatial credit assignment is performed by distributing error spatially across all layers using the chain rule of derivatives, and temporal credit assignment is done by unrolling the network in time and performing backpropagation through time (BPTT) using the same chain rule of derivatives. BPTT works by unrolling all input timesteps. Each time step has its own copy of the network (and weights) and receives an input and produces an output. The outputs from each copy of the network is summed and the loss function is defined on the summed output.

The dynamics of the neuron in the output layer is described by Equation (4), where the leak part is removed ($\lambda = 1$) and the neuron only integrates the input without firing. This eliminates the difficulty of defining the loss function on spike count (Lee et al., 2019).

$$u_i^t = u_i^{t-1} + \sum_j w_{ij} o_j \tag{4}$$

The number of neurons in the output layer is same as the number of categories in the classification task. The output of the network is passed through a softmax layer that outputs a probability distribution. The loss function is defined as the cross-entropy between the true output and the network's predicted distribution.

$$L = -\sum_i y_i log(p_i) \tag{5}$$

$$p_i = \frac{e^{u_i^T}}{\sum_{k=1}^{N} e^{u_k^T}} \tag{6}$$

L is the loss function, y the true output, p the prediction, T the total number of time-steps, u^T the accumulated membrane potential of the neuron in the output layer from all time steps, and N the number of categories in the task. For deeper networks and large number of time steps the truncated version of the BPTT algorithm is used to avoid memory issues. In the truncated version

---

Algorithm 3 Training a SNN with surrogate gradient computed with spike timing. The network is composed of L layers. The training proceeds with mini-batch size ($batch\_size$)

Input: Mini-batch of input (X) - target (Y) pairs, network model (N), initial weights (W), threshold voltage (V)

$U, S, M = InitializeNeuronParameters(X)$ [Algorithm 2]

  // Forward propagation

  for $t=1$ **to** T **do**

    $O_0^t = PoissonGenerator(X)$

    for $l=1$ **to** $L\text{-}1$ **do**

      if $isintance(N_l, [Conv, Linear])$ **then**

        // accumulate the output of previous layer in U, soft reset when spike occurs

        $U_l^t = \lambda U_l^{t-1} + W_l O_{l-1}^t - V_l * O_l^{t-1}$

        // generate the output (+1) if U exceeds V

        $O_l^t = STDB(U_l^t, V_l, t)$

        // store the latest spike times for each neuron

        $S_l^t[O_l^t == 1] = t$

      end

      else if $isintance(N_l, AvgPool)$ **then**

        $O_l^t = N_l(O_{l-1}^t)$

      end

      else if $isintance(N_l, Dropout)$ **then**

        $O_l^t = O_{l-1}^t * M_l$

      end

    end

    $U_L^t = \lambda U_L^{t-1} + W_L O_{L-1}^t$

  end

// Backward Propagation

  Compute $\frac{\partial L}{\partial U_L}$ from the cross-entropy loss function using BPTT

  for $t=T$ **to** 1 **do**

    for $l=L\text{-}1$ **to** 1 **do**

      Compute $\frac{\partial L}{\partial O_l^t}$ based on if N_l is linear, conv, pooling, etc.

      $\frac{\partial L}{\partial U_l^t} = \frac{\partial L}{\partial O_l^t} \frac{\partial O_l^t}{\partial U_l^t} = \frac{\partial L}{\partial O_l^t} * \alpha e^{-\beta S_l^t}$

    end

  end

---

the loss is computed at some time-step t' before T based on the potential accumulated till t'. The loss is backpropagated to all layers and the loss gradients are computed and stored. At this point, the history of the computational graph is cleaned to save memory. The subsequent computation of loss gradients at later time-steps ($2t', 3t', ...T$) are summed together with the gradient at t' to get the final gradient. The optimizer updates the parameters at T based on the sum of the gradients. Gradient descent learning has the objective of minimizing the loss function. This is achieved by backpropagating the error and updating the parameters opposite to the direction of the derivative. The derivative of the loss function w.r.t. to the membrane potential of the neuron in the final layer is described by,

$$\frac{\partial L}{\partial u_i^T} = p_i - y_i \tag{7}$$

In BPTT algorithm to calculate the gradient the internal state from the previous time step (Equation 4) is considered as input for the current time step. Gradient descent updates the network parameters W_{ij} of the output layer as,

$$W_{ij} = W_{ij} - \eta \Delta W_{ij} \tag{8}$$

$$\Delta W_{ij} = \sum_t \frac{\partial L}{\partial W_{ij}^t} = \sum_t \frac{\partial L}{\partial u_i^T} \frac{\partial u_i^T}{\partial W_{ij}^t} = \frac{\partial L}{\partial u_i^T} \sum_t \frac{\partial u_i^T}{\partial W_{ij}^t} \tag{9}$$

where η is the learning rate, and W_{ij}^t represents the copy of the weight used for computation at time-step t. In the output layer the neurons do not generate a spike, so the issue of non-differentiability is not encountered. The update of the hidden layer parameters is described by,

$$\Delta W_{ij} = \sum_t \frac{\partial L}{\partial W_{ij}^t} = \sum_t \frac{\partial L}{\partial o_i^t} \frac{\partial o_i^t}{\partial u_i^t} \frac{\partial u_i^t}{\partial W_{ij}^t} \tag{10}$$

o_i^t is the thresholding function (Equation 3) whose derivative w.r.t to u_i^t is zero everywhere and not defined at the time of spike. The challenge of discontinuous spiking nonlinearity is resolved by introducing a surrogate gradient which is the continuous approximation of the real gradient.

$$\frac{\partial o_i^t}{\partial u_i^t} = \alpha e^{-\beta \Delta t} \tag{11}$$

α and β are constants, Δt is the time difference between the current time step (t) and the last time step the post-neuron generated a spike (t_s). It is an integer value whose range is from zero to the total number of time-steps (T).

$$\Delta t = (t - t_s), 0 < \Delta t < T , \ \Delta t \ \epsilon \ \mathbb{Z} \tag{12}$$

The values of α and β are set depending on the value of T. If T is large β is lowered to reduce the exponential decay so a spike can contribute towards gradients for later time-steps. The value of α is also reduced for large T because the gradient can propagate through many time-steps. The gradient is summed at each time-step and thus a large α value may lead to exploding gradient. The surrogate gradient can be pre-computed for all values of Δt and stored in a look-up table for faster computation. The parameter updates are triggered by the spiking activity but the error gradients are still non-zero for time-steps following the spike time. This enables the algorithm to avoid the 'dead neuron' problem, where no learning happens when there is no spike. Fig. 1 shows the activation gradient for different values of Δt, the gradient decreases exponentially for neurons that have not been active for a long time. In Hebbian models of biological learning the parameter update is activity dependent. This is experimentally observed in STDP learning rule which modulates the weights for pair of neurons that spike within a time window (Song et al., 2000).

3 SNN Weight Initialization

A prevalent method of constructing SNNs for inference is ANN-SNN conversion (Diehl et al., 2015; Sengupta et al., 2019). Since the network is trained with analog activations it does not suffer from the non-differentiablity issue and can leverage the training techniques of ANNs. The conversion process has a major drawback: it requires long time-steps ($\sim$ 2500) during inference as mentioned in Section 1. As there is no provision to optimize the parameters after conversion based on spiking activity, the network can not leverage the temporal information of the spikes. In this work, we propose to use the conversion process as an initialization technique for STDB. The converted weights and thresholds serve as a good initialization for the optimizer and the STDB learning rule is applied for temporal and spatial credit assignment.

Algorithm 1 explains the ANN-SNN conversion process. The threshold voltages in SNN needs to be adjusted based on the ANN weights. Sengupta et al. (2019) showed two ways to achieve this: weight-normalization and threshold-balancing. In weight-normalization the weights are scaled by a normalization factor and threshold is set to 1, whereas in threshold-balancing the weights are unchanged and the threshold is set to the normalization factor. Both have a similar effect and either can be used to set the threshold. We employ the threshold-balancing method and the normalization factor is calculated as the maximum output of the corresponding convolution/linear layer in SNN. The maximum is calculated over a mini-batch of input for all time-steps.

There are several constraints imposed on training the ANN for the conversion process (Sengupta et al., 2019; Diehl et al., 2015). The neuron's are trained without the bias term because the bias term in SNN has an indirect effect on the threshold voltage which increases the difficulty of threshold balancing and the process becomes more prone to conversion loss. The absence of bias term eliminates the use of Batch Normalization (Ioffe & Szegedy, 2015) as a regularizer in ANN since it biases the input of each layer to have zero mean. As an alternative, Dropout (Srivastava et al.,

2014) is used as a regularizer for both ANN and SNN training. The implementation of Dropout in SNN is further discussed in Section 4. The pooling operation is widely used in ANN to reduce the convolution map size. There are two popular variants: max pooling and average pooling. Max (Average) pooling outputs the maximum (average) value in the kernel space of the neuron's activations. In SNN the activations are binary and performing max pooling will result in significant information loss for the next layer, so we adopt the average pooling for both ANN and SNN (Diehl et al., 2015).

3.1 VGG ARCHITECTURE

The threshold balancing is performed for all layers except the input and output layer in a VGG architecture (Simonyan & Zisserman, 2014). The threshold assignment is done sequentially as described in Algorithm 1. For each convolution/linear layer the maximum input[3] to the neuron is computed over all time-steps and set as threshold for that layer. This process is repeated sequentially for each layer. The threshold computation for all layers can not be performed in parallel (in one forward pass) because in the forward method (Algorithm 3) we need the threshold at each time-step to decide if the neuron should spike or not.

3.2 RESIDUAL ARCHITECTURE

Residual architectures (He et al., 2016) introduce shortcut connections between layers that are not next to each other. In order to minimize the ANN-SNN conversion loss various considerations were made by Sengupta et al. (2019). The original residual architecture proposed by He et al. (2016) uses an initial convolution layer with wide kernel (7×7, stride 2). For conversion, this is replaced by a pre-processing block consisting of a series of three convolution layer (3×3, stride 1) with dropout layer in between (Fig. 2). The threshold balancing mechanism is applied to only these three layers and the layers in the basic block have unity threshold.
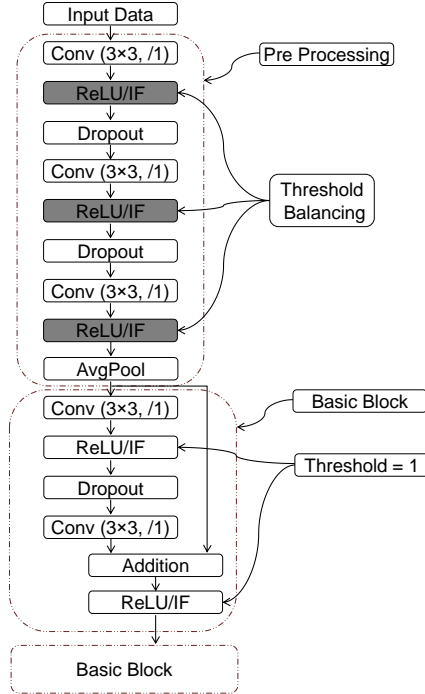

Figure 2: Residual architecture for SNN

4 OVERALL TRAINING ALGORITHM

Algorithm 1 defines the process to initialize the parameters (weights, thresholds) of SNN based on ANN-SNN conversion. Algorithm 2 and 3 show the mechanism of training the SNN with STDB. Algorithm 3 takes as input a mini-batch of input and target pairs, and the network initialized with ANN-SNN conversion including the threshold voltage for all layers. The threshold voltage for all neurons in a layer is same and is not altered in the training process. The neuron parameters (membrane potential (U), and last spike time (S)) are initialized as described in Algorithm 2. For each dropout layer we initialize a mask (M) for every mini-batch of inputs. The function of dropout is to randomly drop a certain number of inputs in order to avoid overfitting. In case of SNN, inputs are represented as a spike train and we want to keep the dropout units same for the entire duration of the input. Thus, a random mask (M) is initialized (Algorithm 2) for every mini-batch and the input is element-wise multiplied with the mask to generate the output of the dropout layer (Lee et al., 2019). The Poisson generator function outputs a Poisson spike train with rate proportional to the pixel value in the input. A random number is generated at every time-step for each pixel in the input image. The random number is compared with the normalized pixel value and if the random number is less than the pixel value an output spike is generated. This results in a Poisson spike train with rate equivalent to the pixel value if averaged over a long time. The weighted sum of the input is

---

[3] input to a neuron is the weighted sum of spkies from pre-neurons $\sum_j w_{ij} o_j$

Table 1: Classification results (Top-1) for CIFAR10, CIFAR100 and ImageNet data sets. Column-1 shows the type of network architecture. Column-2 shows the accuracy obtained in ANN when trained with the constraints described in Section 3. Column-3 shows the accuracy obtained for SNN inference for $T = 2500$ when converted from a ANN with threshold balancing. Column-4 shows the performance of the same converted SNN with lower time-steps and adjusted thresholds. Column-5 is the performance obtained from training the Column-4 network with STDB for less than 20 epochs.

Architecture	ANN	ANN-SNN	ANN-SNN	SNN
CIFAR10				
VGG5	87.88%	87.64% (T=2500)	84.56% (T=75)	**86.91% (T=75)**
VGG9	91.45%	90.98% (T=2500)	87.31% (T=100)	**90.54% (T=100)**
VGG16	92.81%	92.48% (T=2500)	90.2% (T=100)	**91.13% (T=100)**
ResNet8	91.35%	91.12% (T=2500)	89.5% (T=200)	**91.35% (T=200)**
ResNet20	93.15%	92.94% (T=2500)	91.12% (T=250)	**92.22% (T=250)**
CIFAR100				
VGG11	71.21%	70.94% (T=2500)	65.52% (T=125)	**67.87% (T=125)**
ImageNet				
ResNet34	70.2%	65.1% (T=2500)	56.87% (T=250)	**61.48% (T=250)**
VGG16	69.35%	68.12% (T=2500)	62.73% (T=250)	**65.19% (T=250)**

accumulated in the membrane potential of the first convolution layer. The STDB function compares the membrane potential and the threshold of that layer to generate an output spike. The neurons that output a spike their corresponding entry in S is updated with current time-step (t). The last spike time is initialized with a large negative number (Algorithm 2) to denote that at the beginning the last spike happened at negative infinity time. This is repeated for all layers until the last layer. For last layer the inputs are accumulated over all time-steps and passed through a softmax layer to compute the multi-class probability. The cross-entropy loss function is defined on the output of the softmax and the weights are updated by performing the temporal and spatial credit assignment according to the STDB rule.

5 EXPERIMENTS

We tested the proposed training mechanism on image classification tasks from CIFAR (Krizhevsky et al., 2009) and ImageNet (Deng et al., 2009) datasets. The results are summarized in Table 1. The SNNs achieved convergence in less than 20 epochs when initialized with the ANN converted weights.

CIFAR10: The dataset consists of labeled $60,000$ images of 10 categories divided into training ($50,000$) and testing ($10,000$) set. The images are of size 32×32 with RGB channels.

CIFAR100: The dataset is similar to CIFAR10 except that it has 100 categories.

ImageNet: The dataset comprises of labeled high-resolution 1.2 million training images and $50,000$ validation images with 1000 categories.
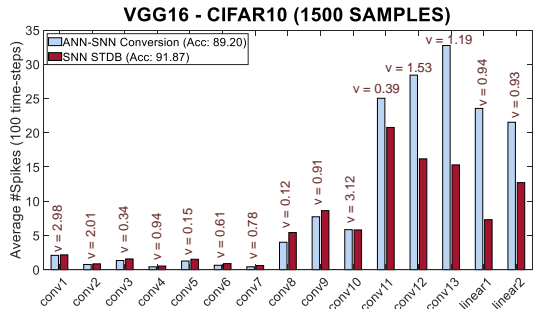

Figure 3: Average number of spikes for each layer in a VGG16 architecture for coverted SNN and SNN trained with STDB.

Table 2: Comparion of our work with other SNN models on CIFAR10 and ImageNet datasets

Model	Dataset	Training Method	Architecture	Accuracy	Time-steps
Hunsberger & Eliasmith (2015)	CIFAR10	ANN-SNN Conversion	2Conv, 2Linear	82.95%	6000
Cao et al. (2015)	CIFAR10	ANN-SNN Conversion	3Conv, 2Linear	77.43%	400
Sengupta et al. (2019)	CIFAR10	ANN-SNN Conversion	VGG16	91.55%	2500
Lee et al. (2019)	CIFAR10	Spiking BP	VGG9	90.45%	100
Wu et al. (2019)	CIFAR10	Surrogate Gradient	5Conv, 2Linear	90.53%	12
This work	**CIFAR10**	**STDB**	**VGG16**	**91.13%** **92.02%**	**100** **200**
Sengupta et al. (2019)	ImageNet	ANN-SNN Conversion	VGG16	69.96%	2500
This work	**ImageNet**	**STDB**	**VGG16**	**65.19%**	**250**

6   ENERGY-DELAY PRODUCT ANALYSIS OF SNNS

A single spike activity in a SNN consumes a constant amount of energy (Cao et al., 2015). The first order analysis of energy-delay product of a SNN is dependent on the number of spikes/inference at each layer and the total number of time-steps. Fig. 3 shows the average number of spikes in each layer when evaluated for 1500 samples from CIFAR10 testset for VGG16 architecture. The average is computed by summing all the spikes in a layer over 100 time-steps and dividing by the number of neurons in that layer. For example, the average number of spikes in 10th convolution layer is 5.8 for both the networks, which implies that over a 100 time-step period each neuron in that layer spikes for 5.8 times on average over all input samples. Higher spiking activity corresponds to lower energy-efficiency. The average number of spikes is compared for a converted SNN and SNN trained with STDB. The SNN trained with STDB has $1.5X$ less number of average spikes over all layers under iso conditions (time-steps, threshold voltages, inputs, etc.). The STDB trained SNN also achieves a higher accuracy compared to the converted SNN. The converted SNNs when simulated for larger time-steps further degrade the energy-delay product with minimal increase in accuracy (Sengupta et al., 2019).

7   RELATED WORK

Bohte et al. (2000) proposed a method to directly train on SNN by keeping track of the membrane potential of spiking neurons only at spike times and backpropagating the error at spike times based on only the membrane potential. This method is not suitable for networks with sparse activity due to the 'dead neuron' problem: no learning happens when the neruons do not spike. In our work, we need one spike for the learning to start but gradient contribution continues in later time-steps as shown in Fig. 1. Zenke & Ganguli (2018) derived a surrogate gradient based method on the membrane potential of a spiking neuron at a single time step only. The error was backpropagated at only one time-step and only the input at that time-step contributed to the gradient. This method neglects the effect of earlier spike inputs. In our approach, the error is backpropagated for every time-step and the weight update is performed on the gradients summed over all time-steps. Shrestha & Orchard (2018) proposed a gradient function similar to the one proposed in this work. They used the difference between the membrane potential and the threshold to compute the gradient

compared to the difference in spike timing used in this work. The membrane potential is a continuous value whereas the spike time is an integer value bounded by the number of time-steps. Therefore, gradients that depend on spike time can be pre-computed and stored in a look-up table for faster computation. They evaluated their approach on shallow architectures with two convolution layer for MNIST dataset. In this work, we trained deep SNNs with multiple stacked layers for complex calssification tasks. Wu et al. (2018) performed backpropagation through time on SNN with a surrogate gradient defined on the membrane potential. The surrogate gradient was defined as piece-wise linear or exponential function of the membrane potential. The other surrogate gradients proposed in the literature are all computed on the membrane potential (Neftci et al., 2019). Lee et al. (2019) approximated the neuron output as continuous low-pass filtered spike train. They used this approximated continuous value to perform backpropagation. Most of the works in the literature on direct training of SNN or conversion based methods have been evaluated on shallow architectures for simple classification problems. In Table 2 we compare our model with the models that reported accuracy on CIFAR10 and ImageNet dataset. Wu et al. (2019) achieved convergence in 12 time-steps by using a dedicated encoding layer to capture the input precision. It is beyond the scope of this work to compute the hardware and energy implications of such encoding layer. Our model performs better than all other models at far fewer number of time-steps.

8 CONCLUSIONS

The direct training of SNN with backpropagation is computationally expensive and slow, whereas ANN-SNN conversion suffers from high latency. To address this issue we proposed a hybrid training technique for deep SNNs. We took an SNN converted from ANN and used its weights and thresholds as initialization for spike-based backpropagation of SNN. We then performed spike-based backpropagation on this initialized network to obtain an SNN that can perform with fewer number of time-steps. The number of epochs required to train SNN was also reduced by having a good initial starting point. The resultant trained SNN had higher accuracy and lower number of spikes/inference compared to purely converted SNNs. The backpropagation through time was performed with surrogate gradient defined using neuron's spike time that captured the temporal information and helped in reducing the number of time-steps. We tested our algorithm on CIFAR and ImageNet datasets and achieved state-of-the-art performance with fewer number of time-steps.

REFERENCES

Guillaume Bellec, Darjan Salaj, Anand Subramoney, Robert Legenstein, and Wolfgang Maass. Long short-term memory and learning-to-learn in networks of spiking neurons. In *Advances in Neural Information Processing Systems*, pp. 787–797, 2018.

Sander M Bohte, Joost N Kok, and Johannes A La Poutré. Spikeprop: backpropagation for networks of spiking neurons. In *ESANN*, pp. 419–424, 2000.

Yongqiang Cao, Yang Chen, and Deepak Khosla. Spiking deep convolutional neural networks for energy-efficient object recognition. *International Journal of Computer Vision*, 113(1):54–66, 2015.

J. Deng, W. Dong, R. Socher, L.-J. Li, K. Li, and L. Fei-Fei. ImageNet: A Large-Scale Hierarchical Image Database. In *CVPR09*, 2009.

Peter U Diehl, Daniel Neil, Jonathan Binas, Matthew Cook, Shih-Chii Liu, and Michael Pfeiffer. Fast-classifying, high-accuracy spiking deep networks through weight and threshold balancing. In *2015 International Joint Conference on Neural Networks (IJCNN)*, pp. 1–8. IEEE, 2015.

Peter U Diehl, Guido Zarrella, Andrew Cassidy, Bruno U Pedroni, and Emre Neftci. Conversion of artificial recurrent neural networks to spiking neural networks for low-power neuromorphic hardware. In *2016 IEEE International Conference on Rebooting Computing (ICRC)*, pp. 1–8. IEEE, 2016.

Kaiming He, Xiangyu Zhang, Shaoqing Ren, and Jian Sun. Deep residual learning for image recognition. In *Proceedings of the IEEE conference on computer vision and pattern recognition*, pp. 770–778, 2016.

Dongsung Huh and Terrence J Sejnowski. Gradient descent for spiking neural networks. In *Advances in Neural Information Processing Systems*, pp. 1433–1443, 2018.

Eric Hunsberger and Chris Eliasmith. Spiking deep networks with lif neurons. *arXiv preprint arXiv:1510.08829*, 2015.

Sergey Ioffe and Christian Szegedy. Batch normalization: Accelerating deep network training by reducing internal covariate shift. *arXiv preprint arXiv:1502.03167*, 2015.

Alex Krizhevsky, Geoffrey Hinton, et al. Learning multiple layers of features from tiny images. Technical report, Citeseer, 2009.

Chankyu Lee, Syed Shakib Sarwar, and Kaushik Roy. Enabling spike-based backpropagation in state-of-the-art deep neural network architectures. *arXiv preprint arXiv:1903.06379*, 2019.

Emre O Neftci, Hesham Mostafa, and Friedemann Zenke. Surrogate gradient learning in spiking neural networks. *arXiv preprint arXiv:1901.09948*, 2019.

Abhronil Sengupta, Yuting Ye, Robert Wang, Chiao Liu, and Kaushik Roy. Going deeper in spiking neural networks: Vgg and residual architectures. *Frontiers in neuroscience*, 13, 2019.

Sumit Bam Shrestha and Garrick Orchard. Slayer: Spike layer error reassignment in time. In *Advances in Neural Information Processing Systems*, pp. 1412–1421, 2018.

Karen Simonyan and Andrew Zisserman. Very deep convolutional networks for large-scale image recognition. *arXiv preprint arXiv:1409.1556*, 2014.

Sen Song, Kenneth D Miller, and Larry F Abbott. Competitive hebbian learning through spike-timing-dependent synaptic plasticity. *Nature neuroscience*, 3(9):919, 2000.

Nitish Srivastava, Geoffrey Hinton, Alex Krizhevsky, Ilya Sutskever, and Ruslan Salakhutdinov. Dropout: a simple way to prevent neural networks from overfitting. *The journal of machine learning research*, 15(1):1929–1958, 2014.

Yujie Wu, Lei Deng, Guoqi Li, Jun Zhu, and Luping Shi. Spatio-temporal backpropagation for training high-performance spiking neural networks. *Frontiers in neuroscience*, 12, 2018.

Yujie Wu, Lei Deng, Guoqi Li, Jun Zhu, Yuan Xie, and Luping Shi. Direct training for spiking neural networks: Faster, larger, better. In *Proceedings of the AAAI Conference on Artificial Intelligence*, volume 33, pp. 1311–1318, 2019.

Friedemann Zenke and Surya Ganguli. Superspike: Supervised learning in multilayer spiking neural networks. *Neural computation*, 30(6):1514–1541, 2018.